# Wigner-Thomas spin precession in polarized coincidence electronuclear scattering

V. Dmitrašinović
*Nuclear and Particle Theory Group, Physics Department, University of the Witwatersrand, P.O. WITS 2050, Johannesburg, South Africa*
(Received 26 May 1992; revised manuscript received 14 October 1992)

The role of the Wigner-Thomas precession in nucleon recoil polarization measurements in coincidence electron scattering processes is examined. The necessary formalism is developed within the framework of the Jacob-Wick method, and then applied to two processes: the pseudoscalar electroproduction off a nucleon and the deuteron two-body electrodisintegration.

PACS number(s): 25.30.−c, 24.70.+s, 13.60.−r

## I. INTRODUCTION AND SUMMARY

The planning and construction of new electron scattering facilities has revived interest in coincidence electronuclear scattering, and in polarization measurements in particular. In recent years we have seen a number of theoretical papers on this issue [1–5]. Most of the papers written so far employed the center-of-mass (c.m.) frame because of the relative simplicity it offers to the theorist. But experiments are done in the laboratory (lab) frame. Hence, if one is to make contact between theory and experiment, one needs explicit Lorentz boost transformation laws for the observables. The transformation properties of the unpolarized structure functions in coincidence electronuclear scattering were worked out by Walecka and Zucker [6] a long time ago, and were recently brought back into the spotlight [1,2,5]. Analogous transformation properties of the polarized structure functions were mentioned in a paper by Dmitrašinović and Gross [2], but were neither derived nor spelled out in detail. In this frankly pedagogical paper, we examine the c.m.→lab boost transformation properties of the coincidence polarized inelastic electron scattering structure functions; in that sense this paper is a followup to Ref. [2].

The difference between the Lorentz boost transformation properties of the unpolarized and polarized structure functions is due to the presence of an explicit specification of the spin state of at least one of the particles. In all other regards the polarized and unpolarized structure functions are identical. The spin state of a particle is specified by a spin density matrix, which in turn can be decomposed into a sum over spherical, or Cartesian, spin-matrix tensors with definite rotational transformation properties. The expansion coefficients themselves have the exactly opposite (inverse) transformation properties under rotations to the tensors multiplying them, resulting in a scalar density matrix. Thus, for particles with spin $\frac{1}{2}$, three expansion coefficients, forming a polarization pseudovector $\mathbf{s}$, are sufficient for the complete description of their polarization states. For higher spin values one needs higher tensor coefficients. In this way we have assigned another (pseudo)vector (tensor) besides the three-momentum $\mathbf{p}$, to the observed particle and, hence, also to the polarized structure function. The spin dependence of the Lorentz boost properties of the polarized structure functions enters through the difference between the Lorentz boost transformation properties of the spin three-vector (tensor) and the momentum three-vector. So we must first determine the Lorentz boost transformation properties of the spin vector (tensor) before we can look at the transformation properties of the polarized structure functions.

In order to do that, we note that, in the rest frame of the particle, the density matrix is normalized: $\mathrm{tr}\rho=1$. It follows that the polarization vector (tensor) is also normalized to unity ($\mathbf{s}^2=1$), in that same frame. Then, one uses the three-vector $\mathbf{s}$ with a vanishing zeroth (time) component $s_0=0$ in the rest frame of the particle as the definition of the covariant polarization four-(pseudo)vector $s^\mu$. This normalized ($s^2=s_\mu s^\mu=-1$) four-vector is clearly spacelike and orthogonal to the four-momentum $p_\mu$ of the particle: $s\cdot p=s_\mu p^\mu=0$. The four-momentum $p_\mu$ is manifestly a dimensional quantity ($p^2=m^2$, where $m$ is the mass of the particle). We introduce the four-velocity $v_\mu=(1/m)p_\mu$ in order to have a dimensionless quantity whose transformation properties can be compared with those of the spin four-vector $s_\mu$. Because of the orthogonality between $v_\mu$ ad $s_\mu$, and their timelike and spacelike natures, respectively, we expect that their Lorentz transformation properties will be very different. So even if the three-vector parts of the two happen to be parallel in some given frame of reference (the c.m. frame in our case), they will not be parallel[1] after a Lorentz boost along an axis different from the direction of motion of the particles. We have thus established that the simple physical reason for the different rotation rates of the three-vector parts of the momentum and the polarization four-vectors under a Lorentz boost is their orthogonality and their timelike and spacelike natures, respectively.

The contents of this paper are as follows. The observable consequences of this so-called Wigner-Thomas pre-

[1]The only known exceptions to this rule are the massless particles. We will not be concerned with them here.

 

cession in coincidence electron scattering processes are determined in Sec. II of this paper, for the polarized $(e,e'\vec{N})$ reactions calculated in the c.m. frame and within the Jacob-Wick [7] helicity formalism.[2] Specifically, it is shown that only the recoil polarization observables are affected by the Wigner-Thomas precession due to the c.m.→lab boost. Then, in Sec. III, the spin precession angle is calculated as a function of the boost parameters involved in two different ways: first following Ref. [9] and in agreement with Ritus [10], second, following Sommerfeld [11], we show that the spin precession angle, with respect to the rotated direction of particle motion, is just the so-called hyperbolic defect of the triangle formed by the three-vector parts of the four-velocities describing the c.m.→lab, c.m.→rest, and the lab→rest boosts. This result is used to show that the total spin rotation angle is always smaller than the three-velocity rotation angle. Finally, in Sec. IV, these general results are applied to the $\vec{N}(\vec{e},e'\vec{N})\pi$ reaction and the numerical results of an illustrative example are shown to be non-negligible, in contrast to the $\vec{d}(\vec{e},e'\vec{N})$ reaction.

## II. FORMALISM

In order to set the notational conventions, we review in Sec. II A the basic results of the polarization observables analysis in $(e,e'N)$ worked out within the Jacob-Wick formalism in Refs. [1,2]. Then, in Sec. II B we work out the general Lorentz boost transformation properties of two-body helicity amplitudes and of the polarization observables in coincidence electron scattering.

### A. Review of the polarization observables in coincidence electron scattering

The general form of the inelastic coincidence electron scattering cross section for arbitrary polarization of the target and/or ejectile, with two particles in the final state, in the "mixed" frame, i.e., with electron variables in the laboratory and the hadronic variables in the center-of-mass frame, is [2]

$$\frac{d^3\sigma}{d\Omega' dE' d\Omega_1}=\frac{\sigma_M p_1}{4\pi M_T}\left\{\left[\frac{W}{M_T}\right]^2 v_L R_L+v_T R_T+v_{TT}[\cos 2\phi\, R_{TT}^{(I)}+\sin 2\phi\, R_{TT}^{(II)}]\right.$$
$$\left.+\left[\frac{W}{M_T}\right]v_{TL}[\cos\phi\, R_{TL}^{(I)}+\sin\phi\, R_{TL}^{(II)}]+2hv'_T R_{T'}+2h\left[\frac{W}{M_T}\right]v'_{TL}[\cos\phi\, R_{TL'}^{(II)}+\sin\phi\, R_{TL'}^{(I)}]\right\}, \tag{1}$$

where $p_1$ is the absolute value of the ejectile three-momentum in the c.m. frame and $E_1$ is the corresponding ejectile energy; $h=\pm\frac{1}{2}$ is the helicity of the incoming electron, $M_T$ is the target-nucleus mass, $\sigma_M$ is the Mott cross section,

$$\sigma_M=\left[\frac{\alpha\cos\frac{1}{2}\theta}{2E\sin^2\frac{1}{2}\theta}\right]^2,$$

and

$$v_L=\left[\frac{Q^2}{q_L^2}\right]^2,\quad v_{TT}=-\frac{1}{2}\left[\frac{Q^2}{q_L^2}\right],$$
$$v_{TL}=-\frac{1}{\sqrt{2}}\left[\frac{Q^2}{q_L^2}\right]\left[\frac{Q^2}{q_L^2}+\tan^2\frac{1}{2}\theta\right]^{1/2},\quad v'_{TL}=-\frac{1}{\sqrt{2}}\left[\frac{Q^2}{q_L^2}\right]\tan\frac{1}{2}\theta,$$
$$v_T=\frac{1}{2}\frac{Q^2}{q_L^2}+\tan^2\frac{1}{2}\theta,\quad v'_T=\tan\frac{1}{2}\theta\left[\frac{Q^2}{q_L^2}+\tan^2\frac{1}{2}\theta\right]^{1/2}.$$

The kinematic variables entering this cross section are the total c.m. energy of the system $W=\sqrt{(P+q)^2}$ (here $P_\mu$ is the target nucleus four-momentum), the negative four-momentum transfer squared $Q^2=-q^2=\mathbf{q}_L^2-\nu^2$, the absolute value of the momentum transfer three-vector in the lab frame $q_L=|\mathbf{q}_L|$, the energy loss $\nu=E-E'$, the initial state electron energy $E$ and the final state electron energy $E'$ in the lab frame, the electron scattering angle $\theta$ in the lab frame, the ejectile opening angle $\theta_1$ in the c.m. frame, and the azimuthal angle $\phi$ (see Fig. 1). Here $\alpha\simeq 1/137$ is the fine structure constant. The only assumptions entering this result are one-photon-exchange approximation and a conserved hadron electromagnetic (EM) current. Parity conservation has not been assumed.

The response functions $R$'s are functions of $W$, $Q^2$, and $\theta_1$, but not of $\phi$, as long as the target polarization is

[2]Similar conclusions, up to phase factors, ought to hold in nonrelativistic polarization formalisms defined in the "mixed frame," such as that of Arenhövel [5]. The formalisms developed in Refs. [3,4] were constructed in the lab frame only, and hence require no additional boosting.

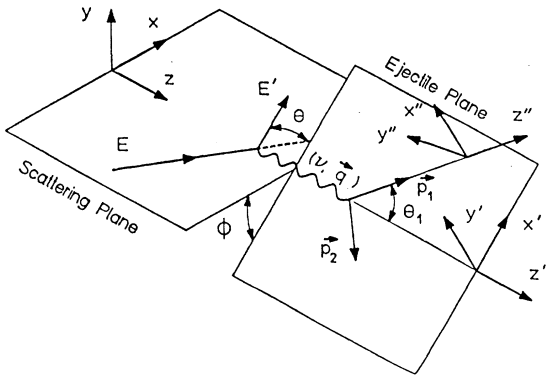


FIG. 1. Geometry of the coincidence electrodisintegration or electroproduction process showing the electron scattering plane, the ejectile plane, and the two coordinate systems in the ejectile plane: $(x',y',z')$ defined by the virtual photon's three-momentum $\mathbf{q}_L$ which is parallel to the $z,z'$ axes, and $(x'',y'',z'')$ where $z''$ is along the ejectile three-momentum $\mathbf{p}_1$. The axes $y',y''$ are perpendicular to the ejectile plane. The axis $y$ is perpendicular to the electron scattering plane.

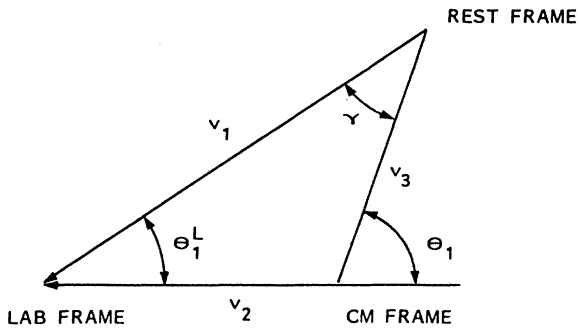


FIG. 2. Diagram representing the three frames of reference discussed in the text connected by the three Lorentz boosts that determine the Wick helicity angle $\omega$; see text. The triangle is not Euclidean, and so the sum of inner angles is different from $\pi$. The angles $\alpha,\beta,\gamma$ are *not* the Euler angles of the Wick-Wigner precession.

specified with respect to the coordinate system $(x',y',z')$ (Fig. 1) and recoil polarization is measured with respect to the $(x'',y'',z'')$ (Fig. 1) coordinate system. The structure functions $R$ are linear combinations of functions $R_{ab}$, which, in turn, are traces of products of helicity transition matrices $\hat{J}_a,\hat{J}_b^\dagger$ [see Eq. (32) of Ref. [2]] and the density matrices of the initial and final states:

$$R_{ab}=4\kappa^2\mathrm{tr}\{\rho_f\hat{J}_a\rho_i\hat{J}_b^\dagger\}\ , \tag{2}$$

where $\kappa=M_1M_2/4\pi^2W$ and $M_{1,2}$ are the masses of the particles number 1 ("ejectile") and 2 ("residual nucleus"), in the final state, respectively. Here the $a,b$ indices stand for the helicities of the virtual photon. The density matrices can be expanded in terms of irreducible tensor operators (ITO's) [see Eqs. (37), (38), and (45) of Ref. [2]]:

$$\rho_{i,f}(j)=\frac{1}{(2S_j+1)}\sum_J\sum_M T^*_{JM}(j)\tau_{JM}(j)\ , \tag{3}$$

where $S_j$ is the spin value of the $j$th particle in the initial or the final state, $\tau_{JM}(j)$ is the $M$th component of the spherical ITO of rank $J$, and $T_{JM}(j)$ are the corresponding components of the *polarization* spherical ITO whose Lorentz boost transformation properties we are seeking. Note that particles No. 2[3] in their respective two-body helicity states (the target particle in the initial state and the "residual nucleus" in the final state) carry a tilde above the polarization ITO in order to indicate this fact.

As pointed out in the Introduction, the spin density matrices are normalized to unity ($\mathrm{tr}\rho=1$) only in the rest frame of the particle. The measurements are done in the lab frame, while the theory is usually calculated in the c.m. frame. Hence, we need the transformation properties of the two-body helicity states under the boost c.m.$\rightarrow$lab (see Fig. 2).

### B. Lorentz boost transformation properties of polarization observables

It has been known for a long time [8,9] that the effect of the three successive Lorentz boosts depicted in Fig. 2 on any one-particle-at-rest state $[p_1^r;\lambda\rangle$ is equivalent to a pure rotation:

$$U^{-1}[h(\mathbf{p}_1^L)]U^{-1}[l]U[h(\mathbf{p}_1)]|p_1^r;\lambda\rangle=R[\mathbf{r}]|p_1^r;\lambda\rangle\ , \tag{4}$$

where $p^r_{1\mu}=(m,\mathbf{0})$ is the four-vector $p_1$ in the rest frame, $h(\mathbf{p}_1)$ is the rest$\rightarrow$c.m. boost, $l$ is the lab$\rightarrow$c.m. boost, and $h(p_1^L)$ is the rest$\rightarrow$lab boost. Here, $\mathbf{p}_1,\mathbf{p}_1^L$ are the ejectile three-momenta in the c.m. and lab frames, respectively. Wick [8] has shown that the application of the three boosts on the left-hand side of Eq. (4) on a one-particle-at-rest state as seen from the c.m. frame leads to a one-particle-at-rest state, as seen from the lab frame. Thus, the relation between the one-body helicity states as viewed from the lab and c.m. frames is a simple rotation:

$$\begin{aligned}&|p_1^r;\lambda\rangle_{\mathrm{lab}}=D^{(s)}_{\lambda'\lambda}[\mathbf{r}]|p_1^r;\lambda'\rangle_{\mathrm{c.m.}}\ ,\\ &\mathbf{r}(l,\mathbf{p}_1)=h^{-1}(\mathbf{p}_1^L)l^{-1}h(\mathbf{p}_1)\ ,\end{aligned} \tag{5}$$

and $D^{(s)}_{\lambda'\lambda}[\mathbf{r}]$ are Wigner rotation matrices[4] of dimension $(2s+1)\times(2s+1)$ for a rotation about the $\hat{\mathbf{r}}$ axis through an angle $\omega=r=|\mathbf{r}|$, with respect to the coordinate frame defined by the direction of motion of the particle. Here $s$ is the spin of the particle and summation over repeated indices is understood. In other words, $\omega$ is the *precession* angle with respect to the *rotated* direction of motion.

[3]For more about "particle No. 2" in the Jacob-Wick formalism, see Sec. II C 1 of Ref. [2].

[4]For a comprehensive review of Wigner matrices, with a detailed comparison of various conventions present in the literature, see Ref. [12]. We keep the Jacob-Wick [7] conventions in this regard (see footnote 11 in Ref. [7]).

This is because, in general, the unit three-vectors $\hat{\mathbf{p}}_1^L$ and $\hat{\mathbf{p}}_1$ that specify the direction of motion are not parallel in two different frames of reference.

Wick [8], MacFarlane [9(b)], and Ritus [10] have written down various formulas describing the angle $\omega$ in terms of three independent boost parameters, but only Ritus' turned out to be useful for our application. In the next section we will concern ourselves with deriving explicit expressions for the Euler angles that describe the rotation vector $\mathbf{r}$ in terms of the boost parameters for $h(\mathbf{p}_1^L), l$ and $h(\mathbf{p}_1)$, and with proving some general properties of these angles. So we leave this topic for now and turn to finding the consequence of this rotation on the polarization observables. First, we work out these consequences for the two-body transition amplitudes, and then use them in the derivation of the polarization observables' transformation properties.

In order to find the Lorentz transformation properties of helicity two-body transition amplitudes $\langle\lambda_3\lambda_4|T|\lambda_1\lambda_2\rangle$, we note that these amplitudes are constructed from direct products of single-particle helicity states sandwiching the Lorentz scalar transition operator $T$. This uniquely determines the transformation law of the amplitudes:

$$\begin{aligned}\langle\lambda_3\lambda_4|T^{\text{lab}}|\lambda_1\lambda_2\rangle &= D^{(s_4)*}_{\lambda_4'\lambda_4}[\mathbf{r}_4]D^{(s_3)*}_{\lambda_3'\lambda_3}[\mathbf{r}_3]\langle\lambda_3'\lambda_4'|T^{\text{c.m.}}|\lambda_1'\lambda_2'\rangle D^{(s_1)}_{\lambda_1'\lambda_1}[\mathbf{r}_1]D^{(s_2)}_{\lambda_2'\lambda_2}[\mathbf{r}_2] \\ &= \langle\lambda_3\lambda_4|D^{(s_3)\dagger}[\mathbf{r}_3]\otimes D^{(s_4)\dagger}[\mathbf{r}_4]T^{\text{c.m.}}D^{(s_1)}[\mathbf{r}_1]\otimes D^{(s_2)}[\mathbf{r}_2]|\lambda_1\lambda_2\rangle\ . \end{aligned} \tag{6}$$

Here, the superscript label on the $T$ matrix indicates the frame of reference in which the matrix element is evaluated. Note that each Wigner $D$ matrix has its own, in principle different from other, rotation vector $\mathbf{r}_j$ which depends on the specifics of the reaction and the kinematics, such as the masses and momenta of the particles and the direction of the boost.

To find the consequences of this transformation law on our observables [Eq. (2)], we remember that these two-body helicity amplitudes form matrices $\hat{J}_a$ and $\hat{J}_b^\dagger$ that appear in the definition of the observables $R_{ab}$ [Eq. (2)]. Use Eqs. (2) and (3) to find, for particle $j=3$ or 4,

$$R_{ab}(T_{JM}(j))=\frac{1}{(2S_j+1)}\text{tr}[\tau_{JM}(j)M_{ab}]\ , \tag{7}$$

where $M_{ab}=\hat{J}_a\rho_i\hat{J}_b^\dagger$ is the "effective density matrix" for particles 1 (the virtual photon) and $j=3$ or 4 (ejectile, or residual nucleus). Similarly, for $j=2$,

$$R_{ab}(\tilde{T}_{JM}(j))=\frac{1}{(2S_j+1)}\text{tr}[\tilde{\tau}_{JM}(j)M'_{ab}]\ , \tag{8}$$

where $M'_{ab}=\hat{J}^\dagger_b\rho_f J_a$ is the "effective density matrix" for particles 1 and $j=2$ (target) and the tilde on $\tilde{T}_{JM}(2)$ denotes the fact that this, just like particle 4 in the final state, is a particle No. 2 in a two-body helicity state. The $j=4$ version of Eq. (7) should also have a tilde. These two-particle "effective density matrices" are just direct products of two one-particle "effective density matrices," whose irreducible components have well-defined transformation properties under rotations. We could rely on the knowledge [12] of those transformation properties and simply write down the transformation properties of the observables, but we give an illustrative example instead. Write $M_{ab}$ out explicitly for $j=3$,

$$\langle\lambda_3|M_{ab}|\lambda_3'\rangle=\sum_{\lambda_4'\lambda_4}\sum_{\lambda_2'\lambda_2}\langle\lambda_3\lambda_4|T|a\lambda_2\rangle\langle\lambda_2|\rho_i|\lambda_2'\rangle\langle b\lambda_2'|T^\dagger|\lambda_3'\lambda_4'\rangle\langle\lambda_4'|\rho f|\lambda_4\rangle\ ,$$

and use Eq. (6), as well as the matrix identity $1=DD^\dagger$ (unitarity of $D$ matrices), to find

$$\langle\lambda_3|M^{\text{lab}}_{ab}|\lambda_3'\rangle=D^{(1)\dagger}_{bd}[r_1]D^{(s_3)\dagger}_{\lambda_3\mu_3}[r_3]\langle\mu_3|M^{\text{c.m.}}_{cd}|\mu_3'\rangle D^{(s_3)}_{\mu_3'\lambda_3'}[r_3]D^{(1)}_{ca}[r_1]\ . \tag{9}$$

Analogous relations for $j=2,4$ are easily derived. Note that Eq. (9) is nothing but a similarity transformation of a matrix with two different kinds of indices, i.e., a direct product of matrices, as advertised. This similarity transformation has exactly the form of an *inverse* rotation [12]. The trace in Eqs. (7) and (8) projects out the $M$th component of the $J$-rank ITO $R^{\text{lab}}_{ab}(T_{JM}(3))$ from $M_{ab}$ for fixed indices $ab$. The matrix $M_{ab}$ can now be written in the form of a sum over products of these coefficients and their corresponding ITO's, just like Eq. (3). The irreducible tensor operators $\tau_{JM}(3)$ have well-known [12] transformation properties under inverse rotations:

$$\tau_{JM}(3)=D^{(J)\dagger}_{M'M}[r_3]\tau_{JM'}(3)\ ,$$

and, as pointed out in the Introduction, the expansion coefficients, in this case the quantities $R^{\text{lab}}_{ab}(T_{JM}(3))$, have exactly the opposite (inverse) transformation properties. Now go back to Eq. (7) and insert Eq. (9) into it, to find the following Lorentz boost transformation laws for $R_{ab}(T_{JM}(3))$:

$$R^{\text{lab}}_{ab}(T_{JM}(3))=D^{(1)\dagger}_{bd}[r_1]D^{(J)}_{M'M}[r_3]R^{\text{c.m.}}_{cd}(T_{JM'}(3))D^{(1)}_{ca}[r_1] \tag{10}$$

and an analogous relation for $R_{ab}(T_{JM}(4))$. In the initial state we have

$$R_{ab}^{\text{lab}}(\tilde{T}_{JM}(2))=D_{bd}^{(1)\dagger}[r_1]D_{M'M}^{(J)}[r_2]R_{cd}^{\text{c.m.}}(\tilde{T}_{JM'}(2))D_{ca}^{(1)}[r_1]\ . \tag{11}$$

In the special case when $\mathbf{r}_{1,2}=0$, as it will turn to be in our electron scattering application, Eqs. (10) and (11) simplify to

$$\begin{aligned} R_{ab}^{\text{lab}}(T_{JM}(3))&=D_{M'M}^{(J)}[r_3]R_{ab}^{\text{c.m.}}(T_{JM'}(3))\ , \\ R_{ab}^{\text{lab}}(\tilde{T}_{JM}(4))&=D_{M'M}^{(J)}[r_4]R_{ab}^{\text{c.m.}}(\tilde{T}_{JM'}(4))\ , \end{aligned} \tag{12}$$

due to the identity $D_{mm'}^{(1)}(\alpha=0,\beta=0,\gamma=0)=\delta_{mm'}$, where $\alpha,\beta,\gamma$ are the Euler angles. Equations (10), (11), and (12) are the principal results of this section.

## III. GENERAL PROPERTIES OF THE WIGNER ROTATION

We are left with the task of evaluating the Euler angles $\alpha,\beta,\gamma$ corresponding to $\mathbf{r}(l,\mathbf{p}_1)$ for various values of $l,\mathbf{p}_1$ in Eqs. (4) and (5). We will proceed along two routes leading to two different-looking, but equivalent, forms of the final result.

### A. Direct evaluation of the spin rotation angle

The first approach is based on the observation that we need not use the defining representation of the Lorentz group, which is four dimensional and cumbersome to work with, to evaluate the rotation vector $\mathbf{r}$ in Eqs. (4) and (5), but we may use a lower-dimensional one. The simplest nontrivial representation is two dimensional[5] and it can be completely specified in terms of Pauli matrices (see Ref. [9]). The boost matrices in this representation are as follows:

$$L(\mathbf{v})=\exp(-i\mathbf{v}\cdot\mathbf{K})=\cosh(\tfrac{1}{2}v)+\hat{\mathbf{v}}\cdot\boldsymbol{\sigma}\sinh(\tfrac{1}{2}v)\ , \tag{13}$$

where $\mathbf{K}=i/2\boldsymbol{\sigma}$, $v=|\mathbf{v}|$, $\hat{\mathbf{v}}=\mathbf{v}/v$, and $\boldsymbol{\sigma}$ are the Pauli matrices. The rotation matrices, on the other hand, are

$$R(\mathbf{r})=\exp(-i\mathbf{r}\cdot\mathbf{J})=\cos(\tfrac{1}{2}r)-i\hat{\mathbf{r}}\cdot\boldsymbol{\sigma}\sin(\tfrac{1}{2}r)\ , \tag{14}$$

where $\mathbf{J}=\frac{1}{2}\boldsymbol{\sigma}$, $r=|\mathbf{r}|$, and $\hat{\mathbf{r}}=\mathbf{r}/r$.

Now insert the explicit two-dimensional representation Eq. (13) of the three relevant boosts, denoting them $v_1\leftrightarrow h^{-1}(\mathbf{p}_1^L)$, $v_2\leftrightarrow l^{-1}$, $v_3\leftrightarrow h^{-1}(\mathbf{p}_1)$, and of the rotation [Eq. (14)] into Eq. (5). It is readily shown [9(a)] that the product of any two boosts $\mathbf{v}_1,\mathbf{v}_2$ can be decomposed into a boost $\mathbf{v}_3$ and a rotation $\mathbf{r}$:

$$L(\mathbf{v}_1)L(\mathbf{v}_2)=R(\mathbf{r})L(\mathbf{v}_3)\ .$$

Multiply this by inverse of $L(v_3)$ from the right and find

$$L(\mathbf{v}_1)L(\mathbf{v}_2)L^{-1}(\mathbf{v}_3)=R(\mathbf{r})\ , \tag{15}$$

which has exactly the same form as Eqs. (4) and (5). By explicit multiplication of these $2\times2$ matrices one obtains eight real (four complex) equations satisfied by the boost and the rotation parameters

$$\begin{aligned} &\cosh(\tfrac{1}{2}v_1)\cosh(\tfrac{1}{2}v_2)+(\hat{\mathbf{v}}_1\cdot\hat{\mathbf{v}}_2)\sinh(\tfrac{1}{2}v_1)\sinh(\tfrac{1}{2}v_2) \\ &\quad=\cos(\tfrac{1}{2}r)\cosh(\tfrac{1}{2}v_3)-i(\hat{\mathbf{r}}\cdot\hat{\mathbf{v}}_3)\sin(\tfrac{1}{2}r)\sinh(\tfrac{1}{2}v_3) \end{aligned} \tag{16}$$

and

$$\begin{aligned} &\hat{\mathbf{v}}_1\sinh(\tfrac{1}{2}v_1)\cosh(\tfrac{1}{2}v_2)+\hat{\mathbf{v}}_2\cosh(\tfrac{1}{2}v_1)\sinh(\tfrac{1}{2}v_2)+i(\hat{\mathbf{v}}_1\times\hat{\mathbf{v}}_2)\sinh(\tfrac{1}{2}v_1)\sinh(\tfrac{1}{2}v_2) \\ &\quad=\hat{\mathbf{v}}_3\cos(\tfrac{1}{2}r)\sinh(\tfrac{1}{2}v_3)-i\hat{\mathbf{r}}\sin(\tfrac{1}{2}r)\cosh(\tfrac{1}{2}v_3)+(\hat{\mathbf{r}}\times\hat{\mathbf{v}}_3)\sin(\tfrac{1}{2}r)\sinh(\tfrac{1}{2}v_3)\ . \end{aligned} \tag{17}$$

There are no constraints between these equations, due to, e.g., unitarity or Hermiticity, because this representation of the Lorentz group is neither unitary nor Hermitian. The imaginary part of the "scalar" equation (16),

$$(\hat{\mathbf{r}}\cdot\hat{\mathbf{v}}_3)\sin(\tfrac{1}{2}r)\sinh(\tfrac{1}{2}v_3)=0\ ,$$

holds for arbitrary value of $r,v_3$ and thus implies

$$\hat{\mathbf{r}}\cdot\hat{\mathbf{v}}_3=0\ .$$

As $\hat{\mathbf{v}}_3$ can point anywhere in the plane defined by $\hat{\mathbf{v}}_1$ and $\hat{\mathbf{v}}_2$, we see that the rotation axis is perpendicular to this plane; i.e., this yields the condition that the rotation be in the "reaction plane," i.e., in the "ejectile plane," of our electron scattering application of Sec. II A. Now take the scalar product of the imaginary part of the "vector" equation (17) with $\hat{\mathbf{r}}$ and find

$$\sinh(\tfrac{1}{2}v_1)\sinh(\tfrac{1}{2}v_2)\sin\gamma_1=-\sin(\tfrac{1}{2}r)\cosh(\tfrac{1}{2}v_3)\ , \tag{18}$$

where $\cos\gamma_1=\hat{\mathbf{v}}_1\cdot\hat{\mathbf{v}}_2$, $\sin\gamma_1=\hat{\mathbf{r}}\cdot(\hat{\mathbf{v}}_1\times\hat{\mathbf{v}}_2)$. Divide this Eq. (18) by the real part of the "scalar" equation (16) to find

[5]This is the defining representation of the Lie group $SL(2,C)$, which has the same Lie algebra as the Lorentz [9(b)] group SO(3,1) and hence the same algebraic properties of its group elements, but different global topological properties ("connectedness"). The way in which these two groups are related to each other is very similar to the way SU(2) and the rotation group SO(3) are related.

$$\tan(\tfrac{1}{2}r)=\frac{-\sinh(\frac{1}{2}v_1)\sinh(\frac{1}{2}v_2)\sin\gamma_1}{\cosh(\frac{1}{2}v_1)\cosh(\frac{1}{2}v_2)+\sinh(\frac{1}{2}v_1)\sinh(\frac{1}{2}v_2)\cos\gamma_1}\ . \tag{19}$$

Note that taking the inverse of Eq. (15) yields

$$L(\mathbf{v}_3)L^{-1}(\mathbf{v}_2)L^{-1}(\mathbf{v}_1)=R^{-1}(\mathbf{r})\ ; \tag{20}$$

i.e., it substitutes $\mathbf{v}_1$ by $-\mathbf{v}_3$ and $\mathbf{v}_2$ by $-\mathbf{v}_2$ on the left-hand side, and it changes the direction of the rotation on the right-hand side of Eq. (15). Multiply both the numerator and the denominator of such an "inverted" Eq. (19) by $\cosh(\frac{1}{2}v_3)\cosh(\frac{1}{2}v_2)$ and then use the half-angle formulas for cosh and sinh. Upon taking into account the change of sign of the rotation in Eq. (19) due to the "inversion" of boosts, we reconstruct Ritus' [10] expression for the spin precession angle $\omega=r$:

$$\tan\left[\frac{\omega}{2}\right]=\frac{\sinh v_2\sinh v_3\sin\theta_1}{(1+\cosh v_2)(1+\cosh v_3)+\sinh v_2\sinh v_3\cos\theta_1}\ , \tag{21}$$

where the boost parameters $v_{2,3}$ are specified below Eq. (14). The relation between the rapidities $v_j$ and the more conventional boost parameters $\beta_j,\gamma_j$ is

$$\gamma_j=\cosh v_j\ ,\quad \gamma_j\beta_j=\sinh v_j\ . \tag{22}$$

Note that Eq. (21) implies that $\omega$ vanishes for $\theta_1=0,\pi$, as promised in Sec. II, which means that boosts parallel to the direction of motion of a particle do not induce a finite spin precession angle $\omega$. This is exactly the case for both of the initial state particles (virtual photon and the target), for the c.m.→lab boost. That means that neither of them experiences a spin precession due to this boost, as advertised in the previous section, and in Sec. II H of Ref. [2].

Note, from Eqs. (4) and (5), that the rotation is defined with respect to the coordinate system defined by the three-momentum of the ejectile in the c.m. frame [in coincidence electron scattering this is the $(x'',y'',z'')$ coordinate system]. The angle $\omega$ is the precession angle of the spin with respect to the coordinate system defined by the direction of motion of the particle, and will be referred to as the Wick-Wigner helicity precession angle.[6] The *total* spin rotation angle $\gamma$ (Fig. 2) is clearly equal to $\theta_1-\theta_1^L-\omega$. Note that this angle $\gamma$ is *not* the Euler angle of the Wick-Wigner presession vector $\mathbf{r}$. Thus, an explicit evaluation of $\mathbf{r}$ in Eqs. (4) and (5) in this representation (i) confirms that it is a rotation; (ii) confirms that the rotation is in the scattering plane determined by the three-vectors $\mathbf{p}_1^L,\mathbf{p}_1$ [ejectile $(x'',z'')$ plane in Fig. 1, in coincidence electron scattering], which is equivalent to setting the corresponding Euler angles $\alpha=\gamma=0$; (iii) gives an explicit formula Eq. (21) for the Wick-Wigner precession angle $\omega$, due to Ritus [10], which confirms that there is no Wick-Wigner precession of the target particle spin direction due to the c.m.→lab boost.

The formula Eq. (21) will be used to evaluate the Wick-Wigner angle in coincidence electron scattering, where $v_2$ is the rapidity of the c.m.→lab boost and $v_3$ corresponds to the c.m.→rest boost.

[6]This angle was called the Wigner angle $\theta_W$, in Ref. [2]; it is also the "hyperbolic defect" (see the next subsection and the extended footnote 7) of the "velocity triangle" on a hyperboloid, corresponding to the boosts depicted in Fig. 2.

### B. Sommerfeld's method

We now present another way of calculating the spin precession angle $\omega$, which is useful for establishing general properties of this angle, especially with respect to the three-velocity rotation angle. The "trick" is to notice that the three boosts involved in Eq. (5) define the addition of four-velocities in special relativity. Next we use the observation of Sommerfeld [11] that the velocity addition theorem in special relativity corresponds to a (non-Euclidean) triangle on a hyperboloid ("sphere of radius $i$").[7] The Wick-Wigner angle is just the hyperbolic defect (the difference between $\pi$ and the sum of inner angles of the triangle) of this velocity triangle. One can use a wide variety of formulas from spherical trigonometry, appropriately modified for hyperbolic trigonometry, to express this angle in terms of any combination of three independent kinematic variables (such as angles or rapidities) describing this velocity triangle.

Starting from the hyperbolic cosine theorem [8] for each of the three angles of the "hyperbolic" triangle,

[7]The meaning of this mysterious-sounding statement is the following: The four-velocity $v_\mu=p_\mu/m$ of a particle of mass $m$ and four-momentum $p_\mu$ and is normalized to unity by construction: $v_\mu^2=p^2/m^2=1$. But this holds for any four-velocity, and so if one adds two four-velocities $v_1$ and $v_2$, the sum $v_3$ has to be normalized too. This imposes strong constraints on the zeroth component of the sum $v_3$. The three-vector components $\mathbf{v}_1$ and $\mathbf{v}_2$ define a plane in the three-dimensional space in which $\mathbf{v}_3$ has to lie too. This allows us to eliminate one (the "perpendicular") component of the three-vector $\mathbf{v}_j$, $j=1,2,3$ from the analysis by defining a coordinate system in which the perpendicular component of *all* three three-velocities is zero. We have thus reduced the full four-dimensional problem to a three-dimensional one. Writing $v_j^0=\cosh u_j=\cos iu_j$ and $\mathbf{v}_j=\hat{\mathbf{v}}_j\sinh u_j=-i\hat{\mathbf{v}}_j\sin iu_j$, in this new coordinate system where $\hat{\mathbf{v}}_j$ is a two-dimensional unit vector in the "velocity plane," we find $i^2=(iv_j^0)^2+(\mathbf{v}_j)^2=(i\cos iu_j)^2+(i\hat{\mathbf{v}}_j\sin iu_j)^2$, i.e., the equation for a three-dimensional sphere of radius $i$. This is Sommerfeld's "sphere of radius $i$" or the relativistic velocity hyperboloid. Thus, in four-velocity space, Fig. 2 is not planar any more, but has a negative curvature and the sum of all inner angles in the triangle is less than $\pi$.

$$\cosh(a)=\cosh(b)\cosh(c)-\sinh(b)\sinh(c)\cos(\alpha)\ ,$$
$$\cosh(b)=\cosh(a)\cosh(c)-\sinh(a)\sinh(c)\cos(\beta)\ , \tag{23}$$
$$\cosh(c)=\cosh(b)\cosh(a)-\sinh(b)\sinh(a)\cos(\gamma)\ ,$$

by simple algebraic manipulation we obtain

$$\sin\left[\frac{\alpha}{2}\right]=\left[\frac{\sinh(s-b)\sinh(s-c)}{\sinh(b)\sinh(c)}\right]^{1/2},\quad \cos\left[\frac{\alpha}{2}\right]=\left[\frac{\sinh(s)\sinh(s-a)}{\sinh(b)\sinh(c)}\right]^{1/2},$$
$$\sin\left[\frac{\beta}{2}\right]=\left[\frac{\sinh(s-a)\sinh(s-c)}{\sinh(a)\sinh(c)}\right]^{1/2},\quad \cos\left[\frac{\beta}{2}\right]=\left[\frac{\sinh(s)\sinh(s-b)}{\sinh(a)\sinh(c)}\right]^{1/2}, \tag{24}$$
$$\sin\left[\frac{\gamma}{2}\right]=\left[\frac{\sinh(s-b)\sinh(s-a)}{\sinh(b)\sinh(a)}\right]^{1/2},\quad \cos\left[\frac{\gamma}{2}\right]\left[\frac{\sinh(s)\sinh(s-c)}{\sinh(b)\sinh(a)}\right]^{1/2},$$

where $s=\frac{1}{2}(a+b+c)$ and $a=v_1, b=v_2, c=v_3$ are the hyperbolic arc lengths corresponding to the sides of the triangle opposite the angles $\alpha=\pi-\theta_1$, $\beta=\theta_1^L$, and $\gamma$, respectively (see Fig. 2). We emphasize once again that the latter are *not* the Euler angles of the Wick-Wigner precession vector **r**, and $\gamma$ used here is the total spin rotation angle from Sec. III B.

Putting these results into formulas for the sine and cosine of $\frac{1}{2}\epsilon$, where $\epsilon=\pi-(\alpha+\beta+\gamma)$, we find

$$\sin\left[\frac{\epsilon}{2}\right]=\frac{\sqrt{1+2\cosh v_1\cosh v_2\cosh v_3-\cosh^2 v_1-\cosh^2 v_2-\cosh^2 v_3}}{4\cosh(\frac{1}{2}v_1)\cosh(\frac{1}{2}v_2)\cosh(\frac{1}{2}v_3)}\ ,$$
$$\cos\left[\frac{\epsilon}{2}\right]=\frac{1+\cosh v_1+\cosh v_2+\cosh v_3}{4\cosh(\frac{1}{2}v_1)\cosh(\frac{1}{2}v_2)\cosh(\frac{1}{2}v_3)}\ . \tag{25}$$

Equations (25) provide yet another formula for the spin precession angle $\omega$: $\omega=\epsilon$. To see this, divide the first of Eqs. (25) by the second one and find

$$\tan\left[\frac{\epsilon}{2}\right]=\frac{\sqrt{1+2\cosh v_1\cosh v_2\cosh v_3-\cosh^2 v_1-\cosh^2 v_2-\cosh^2 v_3}}{1+\cosh v_1+\cosh v_2+\cosh v_3}\ .$$

Then use the first of Eqs. (23),

$$\cosh v_1=\cosh v_2\cosh v_3+\sinh v_2\sinh v_3\cos\theta_1\ ,$$

and insert it into the denominator to obtain the denominator of the Eq. (21). Then do the same to the numerator, to find

$$\sqrt{1+2\cosh v_1\cosh v_2\cosh v_3-\cosh^2 v_1-\cosh^2 v_2-\cosh^2 v_3}$$
$$=\sqrt{(1-\cosh^2 v_2)(1-\cosh^2 v_3)-\sinh^2 v_2\sinh^2 v_3\cos^2\theta_1}=\sinh v_2\sinh v_3\sin\theta_1\ ,$$

which leads immediately to Eq. (21) and thus confirms that $\omega=\epsilon$.

Equations (25) are particularly useful in the investigation of the nonrelativistic limit; in this limit all $\cosh v_i\to 1$, and so we find $\epsilon\to 0$, i.e., $\gamma\to\theta_1-\theta_1^L$. This is equivalent to the statement that there is no spin rotation relative to the momentum, i.e., no Wick-Wigner precession, in the nonrelativistic limit: The spin and the velocity three-vectors remain parallel in that limit.

Note that from Eqs. (25) $\epsilon\geq 0$, or, equivalently, $(\alpha+\beta+\gamma)\leq\pi$ follows. This is because both quantities on the left-hand sides of Eqs. (25) are positive. That also tells us that $\theta_1-\theta_1^L\geq\gamma$, i.e., that, in general, the spin three-vector rotates in the same direction, but more slowly than the momentum three-vector as a consequence of Lorentz boosts.

## IV. APPLICATION TO COINCIDENCE ELECTRON SCATTERING

In this section we apply the general results of Sec. III to the two exclusive polarized inelastic electron scattering processes treated in Refs. [1,2]: the pseudoscalar, or scalar electroproduction off a spin $\frac{1}{2}$ target, and the deuteron two-body electrodisintegration.

We have seen in Sec. III that the in-ejectile-plane (Fig. 1) components of the recoil polarization vector in a $(e,e'\vec{N})$ reaction experience a Wigner-Thomas precession through angle $\omega$ about the axis $y''$ (Fig. 1), while the target and photon spins remain unchanged. The components of the recoil polarization of a spin $\frac{1}{2}$ particle form a polarization vector. Hence they can be recast into the form of a rank-1 ITO. Then Eq. (12) together

with the property of the Wigner $D$ matrices $D^{(J)}_{M'M}(\alpha=0,\beta=\omega,\gamma=0)=d^{(J)}_{M'M}(\omega)$ and the Ref. [12] representation of $d^{(1)}_{M'M}(\omega)$ yield

$$R^{\rm lab}_{ab}(l)=\cos\omega R^{\rm c.m.}_{ab}(l)+\sin\omega R^{\rm c.m.}_{ab}(s)\ ,$$
$$R^{\rm lab}_{ab}(s)=\cos\omega R^{\rm c.m.}_{ab}(s)-\sin\omega R^{\rm c.m.}_{ab}(l)\ , \tag{26}$$
$$R^{\rm lab}_{ab}(t)=R^{\rm c.m.}_{ab}(t)\ ,$$

where $(s,t,l)$ are the $(x'',y'',z'')$ (Fig. 1) components of the recoil polarization vector, respectively, in accord with the notation introduced in Sec. II E of Ref. [2], and $a,b$ are the virtual photon helicity indices. Now we remember that the "true" response functions $R$ appearing in the cross section [Eq. (1)] are linear combinations of these $R_{ab}$'s. It follows that the "true" structure functions obey the same transformation law [Eq. (26)], but with $ab$ standing for the generic structure function indices [e.g., $LT$, (I), etc.]. So the net effect of the c.m.→lab boost on the polarized coincidence electron scattering cross section [Eq. (1)] is the mixing of the "corresponding," i.e., of the same "generic type," structure functions that depend on the ejectile plane ($s$ and $l$) components of the recoil polarization vector, besides the changes already discussed in Sec. II H of Ref. [2]. This should not come as a surprise; we have already seen in Tables X–XII of Ref. [2] that all recoil polarization structure functions fall into two classes: one with nonvanishing $U$ (unpolarized) and $n$ (normal), and vanishing $s$ (sideways) and $l$ (longitudinal) recoil polarization components, and the other class with the role of the two groups interchanged. Now, we see that the $s$ and $l$ components mix due to the c.m.→lab boost.

To determine the Wick-Wigner helicity precession angle using Eq. (21), we need explicit formulas expressing the boost parameters in Eqs. (4) and (22) in terms of the appropriate kinematic variables.

### A. Pion electroproduction

We start with pion electroproduction. The three boosts appearing in Eqs. (4) and (5) can be associated with the boosts in Eq. (15) in this way: $v_1\leftrightarrow h^{-1}(\mathbf{p}_1^L), v_2\leftrightarrow l^{-1}, v_3\leftrightarrow h^{-1}(\mathbf{p}_1)$. The respective boost parameters in this case are

$$-\beta_2=\frac{q_L}{\sqrt{q_L^2+W^2}}\ ,\quad \gamma_2=\left[1+\left[\frac{q_L}{W}\right]^2\right]^{1/2}\ ,$$
$$-\beta_3=\frac{p_1}{E_1}\ ,\quad \gamma_3=\frac{E_1}{M_N}\ , \tag{27}$$
$$-\beta_1=\frac{p_1^L}{E_1^L}\ ,\quad \gamma_1=\frac{E_1^L}{M_N}\ ,$$

where $M_N$ and $m_\pi$ are the nucleon and the pion mass, respectively. The relationship between the lab and c.m. frame opening angles is

$$\cot\theta_1^L=\left[1+\left[\frac{q_L}{W}\right]^2\right]^{1/2}\cot\theta_1+\left[\frac{q_L}{W}\right]\left[\frac{E_1}{p_1}\right]\frac{1}{\sin\theta_1}\ , \tag{28}$$

where

$$p_1=\frac{1}{2W}\sqrt{(W^2-M_N^2-m_\pi^2)-(2M_Nm_\pi)^2}\ ,$$
$$E_1=\frac{1}{2W}(W^2+M_N^2-m_\pi^2)\ . \tag{29}$$

The kinematics of electroproduction is fixed by two independent variables $W$ and $Q^2$. One of them can be substituted by the Bjorken $x$, e.g., the $Q^2$,

$$Q^2=\left[\frac{x}{1-x}\right](W^2-M_T^2)\ , \tag{30}$$

where $x$ is defined by

$$x=\frac{Q^2}{2P\cdot q} \tag{31}$$

for nucleon targets. Direct application of the above results in Eq. (21) leads to the result shown in Figs. 3 and 4.

We see in Figs. 3 and 4 that the spin precession angle $\omega$ is very small for all values of $\theta_1$ in both kinematical situations ($x=0.5$ and 0.75) used here. As expected, $\omega$ vanishes in the forward and backward scattering kinematics, and turns out to be substantially smaller than $\theta_1-\theta_1^L$, in accord with Sommerfeld's general argument, especially in the backward scattering ($\theta_1\simeq 180°$) region. In other words, the Wigner-Thomas precession of the ejected nucleon spin in the $\vec{N}(\vec{e},e'\vec{N})$ reaction is most important at ejectile opening angle $\theta_1\simeq 90°$. A large Wick-Wigner precession angle $\omega$ implies a substantial mixing of the $s$ and $l$ recoil polarization components, or, put differently, that the coordinate axes with respect to which the recoil polarization is measured in the lab frame are not defined by the direction of the ejectile momentum $\mathbf{p}_1^L$ in the lab frame any more, but by a rotated direction. It is not the purpose of this paper to make a systematic exploration of

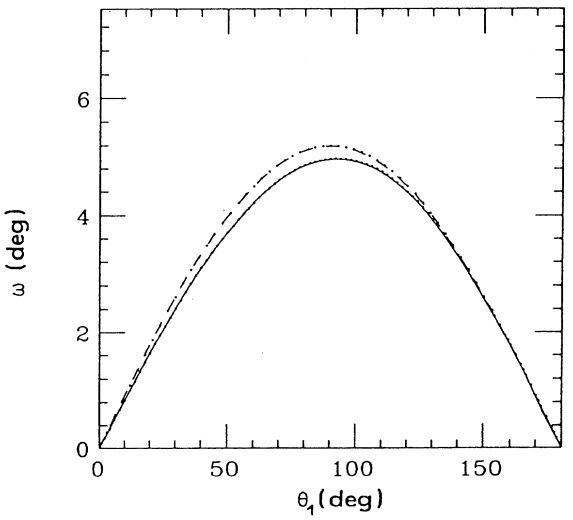


FIG. 3. Wick-Wigner precession angle $\omega$ as a function of the c.m. frame opening angle $\theta_1$, for pion electroproduction off the nucleon at $W=1232$ MeV and Bjorken $x=0.5$ (solid curve), $x=0.75$ (dashed curve).

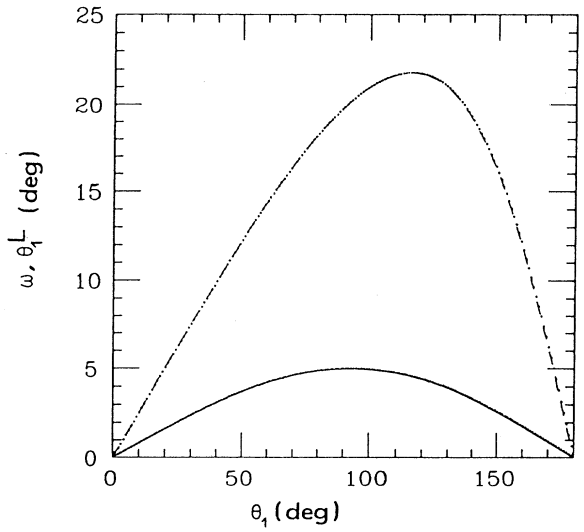


FIG. 4. Wick-Wigner precession angle $\omega$ (solid curve) and the lab frame opening angle $\theta_1^L$ (dashed curve), as functions of the c.m. frame opening angle $\theta_1$, for pion electroproduction off the nucleon at $W=1232$ MeV and Bjorken $x=0.5$.

the size of $\omega$ in various kinematic regions; this will have to be done separately for every experiment.

### B. Deuteron electrodisintegration

The only difference between the pion electroproduction and deuteron electrodisintegration formulas for $\gamma_i$ and $\beta_i$ is in a different expression for $p_1, E_1$ in Eq. (24). For deuteron electrodisintegration the following holds:

$$p_1=\left[\left[\frac{W}{2}-M_N\right]\left[\frac{W}{2}+M_N\right]\right]^{1/2},$$
$$E_1=\tfrac{1}{2}W\ . \tag{32}$$

The use of Eqs. (32) and (27) in Eq. (21) leads to similar results for $\omega$ in deuteron electrodisintegration. We have confined ourselves to the two-body final state deuteron electrodisintegration. This limits the total c.m. energy of the system to $W\leq(2M_N+m_\pi)$ and thus strongly limits the size of $\gamma_3$ to $\gamma_3\leq 1.07$. Hence, the final state nucleons are nonrelativistic and we conclude from the results of Sec. III B that the spin direction essentially rotates together with the nucleon momentum. The same comments hold for heavier target nuclei and heavier ejectiles.

To summarize, we have determined the effects of the c.m.$\rightarrow$lab Lorentz boost on the spin polarization observables in polarized coincidence inelastic electron scattering within the Jacob-Wick helicity formalism. The stated Lorentz boost rotates the two in-ejectile-plane components of the recoil polarization vector observables through angle $\omega$ about the axis perpendicular to the ejectile plane. Two applications of Ritus' formula for $\omega$ were made, to $\vec{N}(\vec{e},e'\vec{N})\pi$ and $\vec{d}(\vec{e},e'\vec{N})N$, and it was found that the relativistic spin rotation plays an important role at large values of the c.m. frame ejectile opening angle in $\pi$ electroproduction, but was negligible in deuteron electrodisintegration below the $\pi$ threshold.

### ACKNOWLEDGMENTS

The author would like to express his gratitude to Professor F. Gross, under whose guidance this work was done, and to Dr. P. Boucher for conversations on the topic of this paper. Financial support by SURA, through CEBAF, and the hospitality of CEBAF are gratefully acknowledged.

[1] V. Dmitrašinović, T. W. Donnelly, and Franz Gross, *Research Program at CEBAF (III), RPAC III,* edited by F. Gross (CEBAF, Newport News, VA, 1988), p. 547; "Report of the CEBAF Out-of-Plane Task Force," in *ibid.* p. 183.

[2] V. Dmitrašinović and Franz Gross, Phys. Rev. C **40**, 2479 (1989); Phys. Rev. C **43**, 1495(E) (1991).

[3] A. Pickelsimer and J. W. van Orden, Phys. Rev. C **40**, 290 (1989).

[4] A. S. Raskin and T. W. Donnelly, Ann. Phys. (N.Y.) **191**, 78 (1989).

[5] H. Arenhövel, W. Leidemann, and E. L. Tomusiak, Z. Phys. A **331**, 123 (1988), as well as H. Arenhövel, Few Body Syst. **4**, 55 (1988); see also W. Fabian and H. Arenhövel, Nucl. Phys. **A314**, 253 (1979).

[6] J. D. Walecka and P. A. Zucker, Phys. Rev. **167**, 1479 (1968).

[7] M. Jacob and G. C. Wick, Ann. Phys. (N.Y.) **7**, 404 (1959); see also Ref. [13], and references cited therein.

[8] G. C. Wick, Ann. Phys. (N.Y.) **18**, 65 (1962).

[9] (a) A. P. Lightman, W. H. Press, R. H. Price, and S. A. Teukolsky, *Problem Book in Relativity and Gravitation* (Princeton University Press, Princeton, NJ, 1975), problems 1.27 and 1.28; (b) A. J. MacFarlane, J. Math. Phys. **3**, 1116 (1962).

[10] V. I. Ritus, Zh. Eksp. Teor. Fiz. **40**, 352 (1961) [Sov. Phys. JETP **13**, 240 (1961)].

[11] A. Sommerfeld, Phys. Z. **10**, 826 (1909); see Sommerfeld's "Gesammelte Schriften," p. 185; A. Sommerfeld, in *Accademia d'Italia, Convegno Fisika Nucleare 1931* (1932), pp. 137–141.

[12] D. A. Varshalovich, A. N. Moskalev, and V. K. Khersonskii, *Quantum Theory of Angular Momentum* (World Scientific, Singapore, 1988).

[13] C. Kuang-Chao and M. I. Shirokov, Zh. Eksp. Teor. Fiz. **34**, 1230 (1958) [Sov. Phys. JETP **7**, 851 (1958)].